

Suppression of coherence degradation due to plasma contribution in high-power supercontinuum generation in coated metallic hollow waveguides

A. Husakou* and J. Herrmann

Max Born Institute for Nonlinear Optics and Short Pulse Spectroscopy
Max Born Str. 2a, D-12489 Berlin, Germany

gusakov@mbi-berlin.de

Abstract: We study the suppression of noise degradation in high-power soliton-induced supercontinuum generation under the influence of plasma contributions in metallic dielectric-coated hollow waveguides. The high coherence of the supercontinuum is related to the coherent seed components formed by the abruptly rising plasma density. We predict the generation of highly coherent supercontinua with two-octave broad spectra and spectral power densities in the range of MW/nm in such waveguides.

© 2018 Optical Society of America

OCIS codes: (030.1640) Coherence; (190.7110) Ultrafast nonlinear optics

References and links

1. J. C. Knight, T. A. Birks, P. S. J. Russell, and D. M. Atkin, "All-silica single-mode optical fiber with photonic crystal cladding," *Opt. Lett.* **21**, 1547-1549 (1996).
2. P. St. J. Russel, "Photonic crystal fibers", *Science* **299**, 358-362 (2003).
3. J. K. Ranka, R. S. Windeler, A. J. Stentz, "Visible continuum generation in air silica microstructure optical fibers with anomalous dispersion at 800nm," *Opt. Lett.* **25**, 25-27 (2000).
4. A. Husakou, J. Herrmann, "Supercontinuum Generation of Higher-Order Solitons by Fission in Photonic Crystal Fibers," *Phys. Rev. Lett.* **87**, 203901 (2001).
5. J. Herrmann, U. Griebner, N. Zhavoronkov, A. Husakou, D. Nickel, J. C. Knight, W. J. Wadsworth, P. St. J. Russell, G. Korn, "Experimental Evidence for Supercontinuum Generation by Fission of Higher-Order Solitons in Photonic Fibers," *Phys. Rev. Lett.* **88**, 173901 (2002).
6. J. M. Dudley, G. Genty, and S. Coen, "Supercontinuum generation in photonic crystal fibers," *Rev. Mod. Phys.* **78**, 1135-1184 (2006).
7. K. L. Corwin, N. R. Newbury, J. M. Dudley, S. Coen, S. A. Diddams, K. Weber, R. S. Windeler, "Fundamental Noise Limitations to Supercontinuum Generation in Microstructure Fiber," *Phys. Rev. Lett.* **90**, 113904 (2003).
8. T. M. Fortier, J. Ye, S. T. Cundiff, R. S. Windeler, "Nonlinear phase noise generated in air-silica microstructure fiber and its effect on carrier-envelope phase," *Opt. Lett.* **27**, 445-447 (2002).
9. N. R. Newbury, B. R. Washburn, K. L. Corwin, R. S. Windeler, "Noise amplification during supercontinuum generation in microstructure fiber," *Opt. Lett.* **28**, 944-946 (2003).
10. A. L. Gaeta, "Nonlinear propagation and continuum generation in microstructured optical fibers," *Opt. Lett.* **27**, 924-926 (2002).
11. X. Gu, M. Kimmel, A. P. Shreenath, R. Trebino, J. M. Dudley, S. Coen, R. S. Windeler, "Experimental studies of the coherence of microstructure-fiber supercontinuum," *Opt. Express* **11**, 2697-2703 (2003).
12. F. Lu, W. H. Knox, "Generation of a broadband continuum with high spectral coherence in tapered single-mode optical fibers," *Opt. Express* **12**, 347-353 (2004).
13. J. N. Ames, S. Ghosh, R. S. Windeler, A. L. Gaeta, S. T. Cundiff, "Excess noise generation during spectral broadening in a microstructured fiber," *Appl. Phys. B* **77**, 279-284 (2003).
14. D. TÜRKE, S. Pricking, A. Husakou, J. Teipel, J. Herrmann, and H. Giessen, "Coherence of subsequent supercontinuum pulses generated in tapered fibers in the femtosecond regime", *Opt. Express* **15**, 2732-2741 (2007).

15. P. D. Drummond, J. F. Corney, "Quantum noise in optical fibers. I. Stochastic equations," J. Opt. Soc. Am. B **18**, 139-152 (2001).
16. Y. Matsuura and J. A. Harrington, "Infrared hollow glass waveguides fabricated by chemical vapor deposition," Opt. Lett. **20**, 2078-2080 (1995).
17. P. J. A. Sazio, A. Amezcua-Correa, C. E. Finlayson, J. R. Hayes, T. J. Scheidemantel, N. F. Baril, B. R. Jackson, D. Won, F. Zhang, E. R. Margine, V. Gopalan, V. H. Crespi, J. V. Badding, "Microstructured Optical Fibers as High-Pressure Microfluidic Reactors", Science **311**, 1583-1586 (2006).
18. A. Husakou and J. Herrmann, "Dispersion control in ultrabroadband dielectric-coated metallic hollow waveguides," Opt. Express **16**, 3834-3843 (2008).
19. H. R. Reiss, "Effect of an intense electromagnetic field on a weakly bound system", Phys. Rev. A **22**, 1786-1813 (1980).

Many applications require light sources which share with a laser its coherent and unidirectional properties but span a much broader spectral range like an electric bulb. Such coherent white-light sources (supercontinuum, SC) was achieved by the application of microstructure fibers (MF)[1, 2]. When a femtosecond pulse with only nJ energy from a laser oscillator is focused into such fiber, a dramatic conversion from narrowband light to two-octaves broad spectra is observed [3]. The SC generation in MFs in the anomalous dispersion range is connected with the splitting of the input pulse into several fundamental solitons, which emit phase-matched non-solitonic radiation [4, 5]. The threshold for this highly efficient mechanism is significantly lower than for self-phase modulation or any other known spectral broadening process. Therefore soliton-induced supercontinuum generation has attracted significant interest and found many important applications ranging from frequency metrology and optical coherence tomography to spectroscopy, confocal microscopy, medicine and others (for an overview see [6]).

For many applications the noise and coherence properties of this octave-spanning white light is of crucial importance. In particular, for pulse compression a shaper is needed to adjust the phases of the different spectral components with respect to each other. Therefore the pulse-to-pulse phase noise of the spectral components is very detrimental for pulse compression. Low-noise supercontinua are also essential for optical frequency metrology, optical coherence tomography, and other applications. Several experimental studies and theoretical simulations have shown that in general the SC coherence is very sensitive to both the fundamental quantum noise and the shot-to-shot pump intensity fluctuations (technical noise) [7-14] These studies have shown that a sufficient level of coherence of the SCs can only be obtained using pulses with a relatively small intensity and durations of about 50 fs or less [7, 11, 13], or for input wavelengths tuned deeper into the anomalous dispersion region[12].

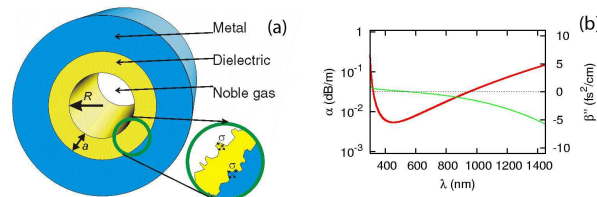


Fig. 1. Scheme (a) and the loss (red curve) and GVD (green curve) in (b) for a silver waveguide with diameter $D = 80 \mu\text{m}$ and fused-silica coating thickness a of 45 nm. The roughness size is indicated by σ .

A further disadvantage of SC generation in MFs is the restricted maximum peak power densities of SCs limited to a range of tens of W/nm due to the small radii in MFs and the material damage of the solid core. Recently we predicted that a significant increase of the peak power

density by up to five orders of magnitude is possible by the use of specific noble-gas-filled hollow waveguides a dielectric-coated metal cladding, which can be produced by chemical vapor deposition [16, 17]. In Fig. 1(a), the geometry of such waveguide is presented. The hollow core of the fibre with diameter D is surrounded by a metallic cladding (blue) coated on the inner side by a dielectric material such as fused silica (yellow) with thickness a .

In the present paper we show that, besides its very high spectral peak power density, soliton-induced SCs in metallic hollow waveguides coated with a dielectric has the additional advantage of suppressed coherence degradation due to the contribution of the plasma.

For the numerical simulations we use a model based on a generalization of the unidirectional equation of Ref. [4] with inclusion of higher-order transverse modes and the effects of the ionization and plasma formation in the waveguide. The Fourier transform $\vec{E}(x, y, z, \omega) = \sum_j F_j(r, \omega) E_j(z, \omega)$ of the electromagnetic field $\vec{E}(z, x, y, t)$ in the waveguide can be decomposed into transverse modes $F_j(r, \omega)$, where j is the mode number, with z being the propagation coordinate and $r^2 = x^2 + y^2$. We consider only linearly-polarized input fields exciting azimuthally-symmetric modes EH_{1j} with the same polarization. Substituting this ansatz into the wave equation and neglecting weak backreflected field components the following system of first-order differential equations can be derived

$$\begin{aligned} \frac{\partial E_j(z, \omega)}{\partial z} = & i\beta_j(\omega)E_j(z, \omega) - \frac{\alpha_j}{2}(\omega)E_j(z, \omega) \\ & + \frac{i\omega^2}{2c^2\epsilon_0\beta_j(\omega)}P_{NL}^{(j)}(z, \omega) \end{aligned} \quad (1)$$

where $\beta_j(\omega)$ and $\alpha_j(\omega)$ are the wavenumber and the loss, $F_j(r, \omega)$ the transverse mode shape and $P_{NL}^{(j)}(z, \omega)$ is the nonlinear polarization of the mode j .

Note that this approach does not use the slowly-varying-envelope approximation which allows to describe adequately the generation of ultrabroadband spectra. The inclusion of higher-order transverse modes takes into account a possible energy transfer to higher-order modes by the nonlinear polarization. $\beta_j(\omega)$, $\alpha_j(\omega)$ and $F_j(r, \omega)$, are calculated by the transfer-matrix approach assuming a circular waveguide structure as shown in Fig. 1(a) of the paper. Additionally, roughness loss is included in the calculation of $\alpha_j(\omega)$ using the model of pointlike scatterers; for further details of the transfer matrix theory and roughness loss calculation, see Ref. [18].

The Fourier transform $P_{NL}^{(j)}(z, \omega)$ of the nonlinear polarization for the transverse mode j is given by

$$P_{NL}^{(j)}(z, \omega) = \int_0^R 2\pi r F_j(r, \omega) \int_{-\infty}^{\infty} \exp(i\omega t) P_{NL}(z, r, t) dr dt \quad (2)$$

where $F_j(r, \omega)$ is the mode profile of the j -th mode. The nonlinear polarization $P_{NL}(z, r, t)$ includes three terms: the Kerr nonlinearity, the plasma-induced refraction index change and absorption due to ionization:

$$\begin{aligned} P_{NL}(z, r, t) = & \epsilon_0 \chi_3 E^3(z, r, t) - \rho(z, r, t) e d(z, r, t) - \\ & E_g \epsilon_0 c \int_{-\infty}^t \frac{E(z, r, t)}{\tilde{I}(z, r, t)} \frac{\partial \rho(z, r, t)}{\partial t} dt \end{aligned} \quad (3)$$

where $\chi_3 = (4/3)c\epsilon_0 n_2$ is the third-order polarizability of the gas filling and $\tilde{I}(z, r, t)$ is the intensity averaged over few optical periods. For argon we have $n_2 = 1 \times 10^{-19} \text{ cm}^2/\text{W}$ at 1 atm, E_g is the ionization potential, $\rho(z, r, t)$ is the electron density and $d(z, r, t)$ is the mean free-electron displacement in the electric field. The evolution of the two latter quantities is described by

$$\frac{\partial \rho(z, r, t)}{\partial t} = (N_0 - \rho(z, r, t)) \Gamma(\tilde{I}(z, r, t)) \quad (4)$$

$$\frac{\partial^2 d(z, r, t)}{\partial t^2} = -eE(z, r, t)/m_e - \frac{\partial_t d(z, r, t)}{\rho(z, r, t)} \frac{\partial \rho(z, r, t)}{\partial t} \quad (5)$$

where $\Gamma(\tilde{I}(z, r, t))$ is the photoionization rate calculated from the Keldysh-Faisal-Reiss model[19] which describes both the multiphoton and tunnelling regime and N_0 is the initial argon density. In the following we study the coherence degradation of the supercontinua due to the influence of the fundamental quantum noise. In the Wigner quasi-probability representation the evolution equations for quantum field operators are mapped onto the classical equations [15] where the effect of quantum noise is included by adding to the input field $E(t)$ the quantum shot noise $\Delta E(t)$ defined by $\langle \Delta E(t_1) \Delta E(t_2) \rangle = \delta(t_1 - t_2) \hbar \omega_0 / (2E_{tot})$ where ω_0 is the input frequency, E_{tot} is the total energy of the pulse and the average $\langle \dots \rangle$ is taken over the noise realisations (see Ref. [15] for details). The quantity which characterizes the coherence of the SC is given by the first order coherence function $g(\lambda)$ which directly corresponds to the visibility measured in interference experiments and is defined as

$$g(\lambda) = \Re \left[\frac{\langle E_b(\lambda) E_a^*(\lambda) \rangle_{ab, a \neq b}}{\langle E_a(\lambda) E_a^*(\lambda) \rangle_a} \right] \quad (6)$$

where $E_a(\lambda)$ is the spectrum in the fundamental mode after the waveguide and the indices a, b denote the realization.

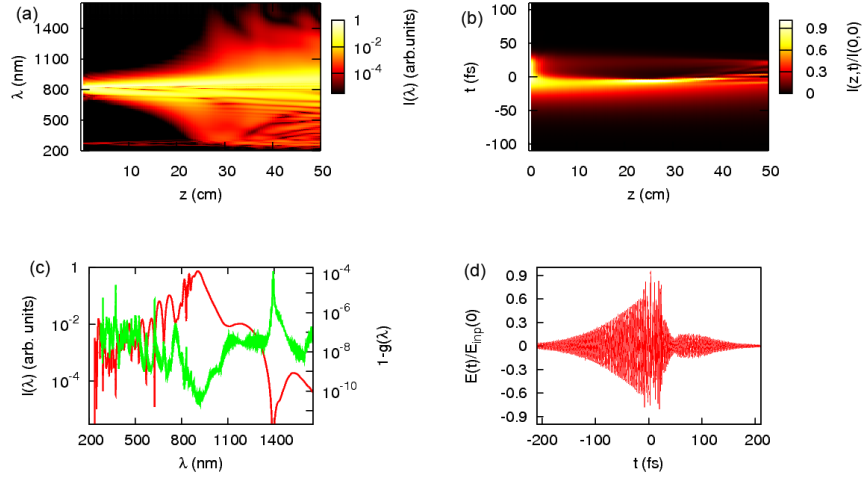


Fig. 2. Evolution of the spectrum (a) and temporal shape (b) for the propagation of a 100-TW/cm², 100-fs pulse in a fused-silica-coated silver waveguide. In (c) the output spectrum (red) and incoherence $1 - g(\lambda)$ (green) are shown and in (d) the output temporal shape are presented. The propagation length is 50 cm, input wavelength is 800 nm, the waveguide parameters are $D = 80 \mu\text{m}$, $a = 45 \text{ nm}$.

We consider a hollow waveguide with a diameter of $80 \mu\text{m}$, which is made from a silver cladding coated from the inner side by a 45-nm-thick layer of fused silica [Fig. 1(a)]. The loss and dispersion properties of the waveguide are illustrated in Fig. 1(b). It can be seen in Fig. 1(b) that the loss remains relatively low in the range of 10^{-2} - 10^{-1} dB/m for wavelengths from $0.4 \mu\text{m}$ to $1.4 \mu\text{m}$. This means that at most 10% of the energy is lost during a propagation over 1 m, while in a conventional dielectric hollow waveguide with the same diameter, roughly 80% of the energy is lost. The physical reason for this difference is that the reflection coefficient for grazing incidence of light is higher for fused-silica-coated silver than for a layer of fused silica. Therefore the diameter of the waveguides can be reduced, which leads to a significant

modification of the dispersion properties and an extended range of anomalous dispersion[18]. The group velocity dispersion, illustrated in Fig. 1(b) by the green curve, is anomalous for $\lambda > 570$ nm at 1 atm of the argon filling.

We now study the evolution of a 100-fs input pulse at 830 nm with a peak intensity of 100 TW/cm² propagating a distance of 50 cm in the above-described fiber. It can be seen in Fig. 2(a),(c) that the generated radiation after 50 cm of propagation covers the spectral range from 200 nm to 1400 nm, with a total width corresponding to more than two octaves. In Fig. 2(b) the evolution of the temporal shape of the pulse is illustrated, which shows pulse compression and formation of an edge in the middle of the pulse with sharply decreasing intensity after the edge. During further propagation distances isolated temporal peaks start to form, as shown in Fig. 2(d). These peaks can be identified as fundamental solitons caused by the anomalous dispersion at the input wavelength together with the Kerr nonlinearity of the argon filling. Similar to the case of soliton-induced SC generation in MFs [4] the two-octave broad spectrum represented by the red curve in Fig. 2(c) comprise the spectrum of several solitons red-shifted by the recoil effect and at the short-wavelength side the non-solitonic radiation emitted by them. The wavelength-averaged peak power spectral density is about 10⁶ W/nm with an intensity at the output of about 10¹⁴ W/cm². In Fig. 2(c) the quantity $1 - g(\lambda)$ (first-order incoherence) is shown by the green curve demonstrating a surprisingly high coherence which deviates from unity by no more than 10⁻⁵. This high coherence of soliton-induced SC generation in hollow waveguides is in contrast to SC generation in MFs based on the same broadening mechanism.

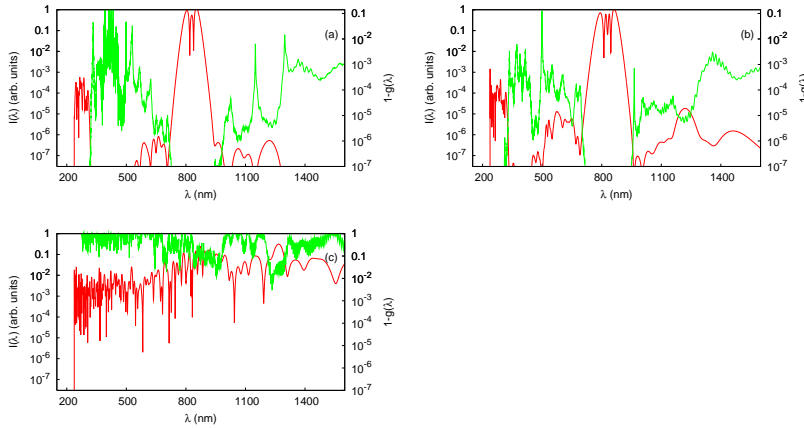


Fig. 3. Spectrum and coherence for a propagation model without plasma contribution. The spectrum (red curve) and coherence (green curve) are presented at the distances of 15 cm (a), 20 cm (b) and 50 cm (c). The input pulse and waveguide parameters are the same as in Fig. 2.

To understand the suppression of coherence degradation for soliton-induced SC generation in metallic hollow waveguide we study the role of the plasma contribution in the SC formation process. In Figs. 3 and 4 we present the evolution of the spectrum and incoherence function $1 - g(\lambda)$ for models without (Fig. 3) and with (Fig. 4) plasma contributions. It can be seen that without plasma, at the propagation length of 15 and 20 cm seed spectral components are formed [Fig. 3(a) and (b)] within spectral wings between 500 nm and 700 nm as well as around 1100 nm. They arise by the amplification of noise due to the gain of the modulation instability. The coherence of the side maxima decreases with propagation from 15 to 30 cm, with an incoherence on the level of 10⁻⁴-10⁻³. With further propagation after fission of the pulse into several solitons, the spectrum is dramatically broadened as shown by the red curve in Fig. 3(c),

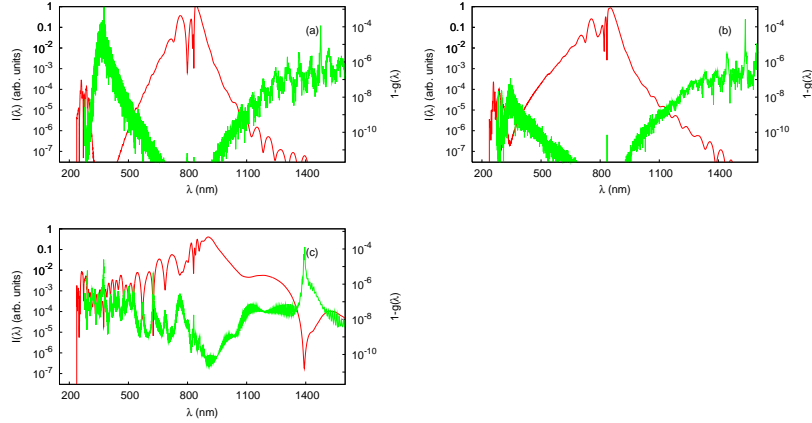


Fig. 4. Spectrum and coherence for a propagation model with plasma contribution. The spectrum (red curve) and coherence (green curve) are presented at the distances of 15 cm (a), 20 cm (b) and 50 cm (c). The input pulse and waveguide parameters are the same as in Fig. 2.

but the coherence is also significantly degraded (green curve) with a low average coherence of the output spectrum $\overline{g(\lambda)} = 0.63$. In contrast, in the case when the plasma contribution is included in the numerical model (Fig. 4), the seed components arise mainly on the short-wavelength side of the spectrum, forming a smooth spectral wing from 300 to 700 nm in Fig. 4(b). The mechanism of this smooth short-wavelength wing formation is related to the abrupt rise of the plasma density near the peak of the pulse leading to a strong phase modulation due to time-dependent plasma contribution in the refractive index. We note that this wing is highly coherent in our case with $1 - g(\lambda) \sim 10^{-9}$ [green curve in Fig. 4(b)], as should be expected since its spectral phase is determined by the phases of the input pulse, similar to the case of self-phase modulation. Now in contrast with Fig. 3(c) further propagation and spectral broadening of the pulse up to 50 cm do not lead to a dramatic coherence degradation but to the preservation of the high coherence of the SC. The resulting spectrum [Fig. 4(c) and Fig. 2(c)] is characterised by the average coherence of $\overline{g(\lambda)} = 1 - 3 \times 10^{-6}$.

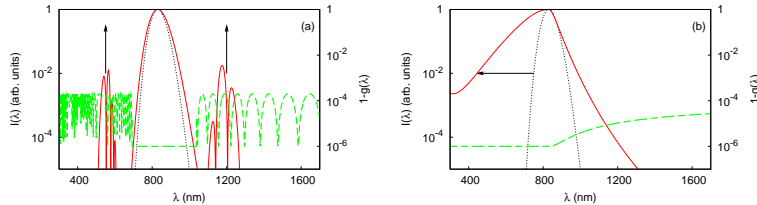


Fig. 5. Schematic presentation of the supercontinuum generation at the initial stage. Black dotted curve indicates the input spectrum, the red curve is the spectrum at the position of the seed component formation, green dashed curve is the incoherence $1 - g(\lambda)$. In (a), arrows indicate the four-wave-mixing gain bands; in (b), the arrow indicates the spectral broadening induced by plasma.

The mechanism of the suppression of coherence degradation in soliton-induced SC generation is schematically presented in Fig. 5(a,b). In the case of a relatively long and intense pulse due to gain by modulation instability seed spectral components arise *from noise*, as represented in Fig. 5(a) by the black arrows. These seed components are further amplified by the gain

produced by the fundamental solitons after fission due to third-order dispersion leading to the large spectral broadening but accompanied by coherence degradation. In contrast, in the case of the seed components formation due to plasma, as schematically presented in Fig. 5(b) the short-wavelength wing arise *from the pulse itself*. It is smooth and highly coherent, and after amplification by the gain which leads to the emission of non-solitonic radiation the coherence remains high.

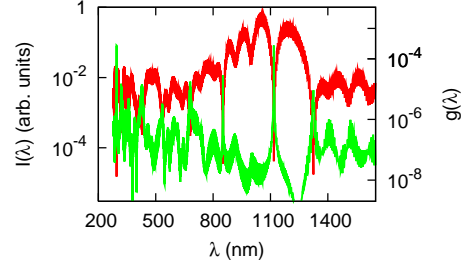


Fig. 6. Output spectrum (red) and coherence (green) for the propagation of a $100\text{-TW}/\text{cm}^2$, 10-fs pulse in a fused-silica-coated silver waveguide. The propagation length is 50 cm, input wavelength is 800 nm, the waveguide parameters are $D = 80 \mu\text{m}$, $a = 45 \text{ nm}$.

For comparison we calculated the spectrum and coherence function for a shorter input pulse, as illustrated in Fig. 6. The spectrum in this case is not significantly broader although slightly smoother, and the coherence increases to values in the range of $1 - 10^{-7}$. In this case the input spectrum is already quite broad, which facilitates the formation of the coherent sidebands from the broad spectrum during the soliton compression and leads to high final coherence.

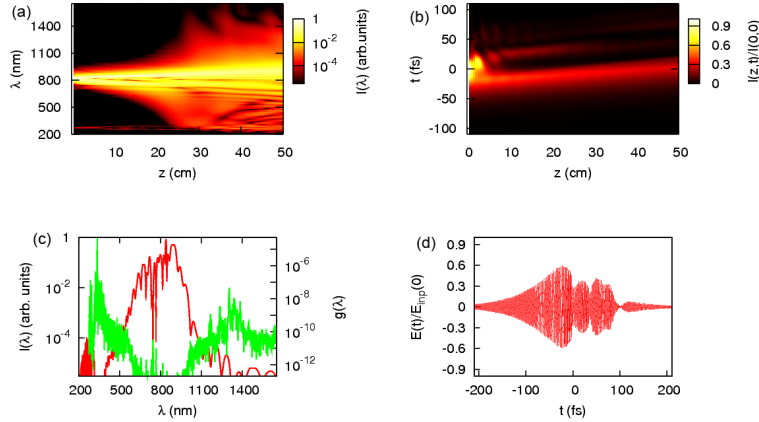


Fig. 7. Evolution of the spectrum (a) and temporal shape (b) for the propagation of a $100\text{-TW}/\text{cm}^2$, 100-fs pulse in a fused-silica-coated silver waveguide. In (c) the output spectrum (red) and the coherence (green) are shown and in (d) the output temporal shape are presented. The propagation length is 50 cm, input wavelength is 800 nm, the waveguide parameters are $D = 200 \mu\text{m}$, $a = 45 \text{ nm}$.

Finally, we have also performed simulations for a larger waveguide diameter of $200 \mu\text{m}$ with smaller waveguide contribution to dispersion and normal GVD at the input wavelength. The results are presented in Fig. 7. In the temporal shape shown in Fig. 7(b),(d) a modulation is formed but without sharp edge, and the spectrum shown in Fig. 7(a) and (c) broadens somewhat

but remains relatively narrow. This indicates that the anomalous dispersion and the soliton mechanism are essential for the predicted two-octave spectral broadening in the considered hollow waveguide, which can not be achieved by self-phase modulation and plasma-related broadening. The coherence shown by the green curve in Fig. 7(c) is very high, typical for spectral broadening by SPM.

In conclusion, we studied the generation of high-power soliton-induced supercontinua in the anomalous dispersion range of metallic dielectric-coated hollow waveguides filled with argon under the influence of plasma contributions to the spectral broadening process. We predicted that the coherence degradation in soliton-induced SC generation as typically observed in MFs can be suppressed by the plasma contributions. The coherence preservation is explained by the formation of seed components of the SC generation due to sharp raise of the plasma density. In this way highly coherent supercontinua with two-octave broad spectra and spectral power densities in the range of MW/nm can be achieved in such waveguides. These findings could have applications in a wide range of fields in which coherent high-power supercontinua are required.